2015

Visualizing superconductivity in FeSe nanoflakes on SrTiO3 by scanning tunneling microscopy

Zhi Li
Chinese Academy of Sciences, zhili@uow.edu.au

Jun-Ping Peng
Hunan University , Chinese Academy Of Sciences

Hui-Min Zhang
Chinese Academy of Sciences

Canli Song
Collaborative Innovation Center Of Quantum Matter, Tsinghua University

Shuaihua Ji
Tsinghua University, Collaborative Innovation Center Of Quantum Matter

See next page for additional authors

Publication Details

Li, Z., Peng, J., Zhang, H., Song, C., Ji, S., Wang, L., He, K., Chen, X., Xue, Q. & Ma, X. (2015). Visualizing superconductivity in FeSe nanoflakes on SrTiO3 by scanning tunneling microscopy. Physical Review B: Condensed Matter and Materials Physics, 91 060509-1-060509-5.

Visualizing superconductivity in FeSe nanoflakes on SrTiO3 by scanning tunneling microscopy

Abstract
Scanning tunneling microscopy and spectroscopy have been employed to investigate the superconductivity in single unit-cell FeSe nanoflakes on SrTiO3 substrates. We find that the differential conductance dI/dV spectra are spatially nonuniform and fluctuate within the flakes as their area is reduced to below ~150 nm2. An enhancement in the superconductivity-related gap size as large as 25% is observed. The superconductivity behavior disappears when the FeSe nanoflakes reduce to ~40 nm2. Compared to a previous report [Wang et al., Chin. Phys. Lett. 29, 037402 (2012)], the gap is asymmetric relative to the Fermi energy EF. All the features, particularly the fluctuating gap and quenched superconductivity, could be accounted for by quantum size effects. Our study helps to understand nanoscale superconductivity in low-dimensional systems.

Keywords
scanning, srtio3, microscopy, nanoflakes, tunneling, fese, superconductivity, visualizing

Publication Details
Li, Z., Peng, J., Zhang, H., Song, C., Ji, S., Wang, L., He, K., Chen, X., Xue, Q. & Ma, X. (2015). Visualizing superconductivity in FeSe nanoflakes on SrTiO3 by scanning tunneling microscopy. Physical Review B: Condensed Matter and Materials Physics, 91 060509-1-060509-5.

Authors
Zhi Li, Jun-Ping Peng, Hui-Min Zhang, Canli Song, Shuaihua Ji, Lili Wang, Ke He, Xiaowei Chen, Qi-Kun Xue, and Xu-Cun Ma

PHYSICAL REVIEW B **91**, 060509(R) (2015)

Visualizing superconductivity in FeSe nanoflakes on $SrTiO_3$ by scanning tunneling microscopy

Zhi Li,[1] Jun-Ping Peng,[1] Hui-Min Zhang,[1] Can-Li Song,[2,3,*] Shuai-Hua Ji,[2,3] Lili Wang,[2,3] Ke He,[2,3] Xi Chen,[2,3] Qi-Kun Xue,[2,3] and Xu-Cun Ma[1,2,3,†]

[1]*State Key Laboratory for Surface Physics, Institute of Physics, Chinese Academy of Sciences, Beijing 100190, China*

[2]*State Key Laboratory of Low-Dimensional Quantum Physics, Department of Physics, Tsinghua University, Beijing 100084, China*

[3]*Collaborative Innovation Center of Quantum Matter, Beijing 100084, China*

(Received 5 October 2014; revised manuscript received 24 January 2015; published 27 February 2015)

Scanning tunneling microscopy and spectroscopy have been employed to investigate the superconductivity in single unit-cell FeSe nanoflakes on $SrTiO_3$ substrates. We find that the differential conductance dI/dV spectra are spatially nonuniform and fluctuate within the flakes as their area is reduced to below $\sim$150 nm^2. An enhancement in the superconductivity-related gap size as large as 25% is observed. The superconductivity behavior disappears when the FeSe nanoflakes reduce to $\sim$40 nm^2. Compared to a previous report [Wang *et al.*, Chin. Phys. Lett. **29**, 037402 (2012)], the gap is asymmetric relative to the Fermi energy E_F. All the features, particularly the fluctuating gap and quenched superconductivity, could be accounted for by quantum size effects. Our study helps to understand nanoscale superconductivity in low-dimensional systems.

DOI: 10.1103/PhysRevB.91.060509 PACS number(s): 68.37.Ef, 74.70.Xa, 74.55.+v, 74.78.−w

I. INTRODUCTION

Superconductivity in reduced dimensions, including ultrathin films [1–3], nanowires [4], and nanograins [5–10], is still a hot topic of interest due to its potential for developing dissipationless nanoelectronics. However, as the size of a superconductor is shrunk to the nanoscale, quantum size effects (QSEs) would become important and can dramatically change its superconducting properties. Many fascinating phenomena, such as the parity effect and shell effect on gap magnitude Δ, have been predicted theoretically [11–13] and ascertained experimentally in several conventional BCS-type superconductors [5–8,10]. Superconductivity can be eventually quenched if the nanograin size is small enough so that the QSE induced discrete energy level spacing [$\sim 2\pi^2\hbar^2/(mk_FV)$] exceeds the bulk gap magnitude Δ_0, where $\hbar$,m,k_F, and V denote the reduced Planck constant, the mass of an electron, the Fermi wave vector, and nanograin volume, respectively. In order to study these phenomena, nanostructures with extremely small k_FV are particularly interesting. Compared to conventional metal superconductors [1–8,10], the layered superconducting compounds (e.g., cuprates and iron-based superconductors) generally exhibit a smaller k_F and represent ideal systems to test the intriguing superconductivity in confined systems. However, the fabrication of small layered superconductors still remains a great experimental challenge.

The recently discovered single unit-cell (UC) FeSe/$SrTiO_3$ films, with a simple crystal structure and a high transition temperature T_c [14–16], have sparked considerable research efforts aimed at uncovering the electron pairing mechanism in high-T_c superconductors, such as extensive angle-resolved photoemission spectroscopy [17–19], theoretical [20,21], and even *in situ* transport studies [22]. Meanwhile, the system provides a platform for exploring QSEs on unconventional superconductivity, given that the electron confinement has already been reached along the z direction. A recent theoretical work has also predicted QSE induced T_c enhancement in iron-based superconductors [23]. So far, T_c enhancement has been observed in FeSe encapsulated in a carbonaceous shell, which was ascribed to the FeSe lattice compression effect [24,25], rather than QSEs.

In this Rapid Communication, we report on scanning tunneling microscopy (STM) and spectroscopy (STS) studies of single UC FeSe nanoflakes on a $SrTiO_3$ substrate grown by molecular beam epitaxy (MBE). The technique allows for a direct probing of the superconducting order parameter and a study of its relationship with lateral QSEs. We find that (i) the gap magnitude Δ fluctuates with flake area A with a maximum value of 25 meV, larger than the previously reported value of 20.1 meV [14], (ii) the superconductivity completely disappears as the nanoflake size A is reduced below $\sim$40 nm^2, and (iii) the gap exhibits great asymmetry with respect to the Fermi energy E_F. We show that the observations are intimately correlated with the lateral QSEs in FeSe nanoflakes.

II. EXPERIMENT

Our experiments were performed on an ultrahigh vacuum low temperature STM (Unisoku) system with a base pressure of 5×10^{-11} Torr, which is connected to a MBE chamber for *in situ* sample preparation. Nb-doped (0.5 wt%) $SrTiO_3$ was etched by Se molecular flux and then used as a substrate for single UC FeSe film growth [14]. The MBE growth of FeSe films has been described in detail elsewhere [26]. Prior to STM/STS measurements at 4.5 K, a polycrystalline PtIr tip was first cleaned by electron-beam heating in the MBE chamber, and then calibrated with Ag/Si(111) films. Unless otherwise noted, tunneling spectra were acquired by disrupting the feedback circuit at a setpoint voltage $V_s = 50$ mV and $I = 50$ pA, sweeping the sample voltage V_s, and extracting the differential tunneling conductance dI/dV using a standard lock-in technique with a small bias modulation of 0.1 mV at 987.5 Hz.

III. RESULTS AND DISCUSSIONS

Figure 1(a) depicts a typical single UC FeSe film grown on a $SrTiO_3$ substrate. The dark trenches divide the films into many

*clsong07@mail.tsinghua.edu.cn
†xucunma@mail.tsinghua.edu.cn

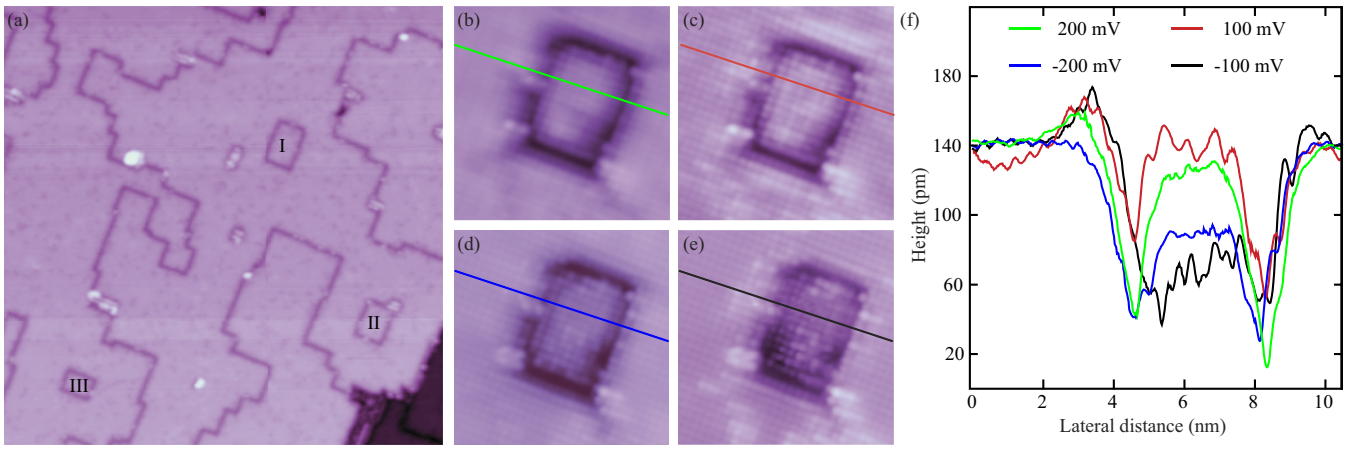

FIG. 1. (Color online) (a) STM topographic image ($V_s = 4$ V, $I = 20$ pA, 100×100 nm) of single UC FeSe films grown on a $SrTiO_3$ substrate. The dark trenches are primarily caused by missing atoms. (b)–(e) STM topographies ($I = 30$ pA, 10×10 nm) in the vicinity of an isolated rectangular FeSe nanoflake, and (f) cross-section height profiles along the straight lines in (b)–(e) at different sample voltages V_s. The bright spots in (b)–(e) correspond to the topmost Se atoms.

domains, as already interpreted before [27]. Occasionally, certain trenches connect together and can completely isolate some rectangular nanoflakes (marked by I, II, and III) from the remaining FeSe films. The rectangular flakes vary from several tens to several hundreds of nm^2 in area. Our careful inspection reveals that the FeSe nanoflakes differ from the continuous films in their electronic structure, as illustrated in Figs. 1(b)–1(f). The apparent height of the nanoflakes usually exhibits a lower value, especially at small and negative (filled states) sample voltages V_s [for example, see Fig. 1(f)]. This suggests that the FeSe nanoflakes are electronically isolated from the other regions, which enables us to detect experimentally their superconductivity. In other words, the isolated FeSe nanoflakes can serve as an ideal system for studying the interplay between lateral QSE and superconductivity.

Below we focus on the dependence of the superconductivity on the nanoflake area A. Figure 2(a) shows a typical superconducting gap taken on a larger FeSe nanoflake ($A > 900$ nm^2), where two E_F-symmetric superconducting coherence peaks at $\sim\pm 16.5$ meV are clearly evident. It is worth noting that these spectra are spatially uniform over different regions of the flake, which resemble those previously reported on FeSe films in a prominent manner [16]. The gap magnitude of $\sim$16.5 meV, most frequently observed, is quite in line with previous measurements [16–19]. As A is reduced, however, the spectra gradually become site dependent, as shown in Fig. 2(b). Two intriguing features are immediately discernible. One is that Δ becomes spatially inhomogeneous and exhibits a maximum value of $\sim$25 meV [black curves in Fig. 2(b)], 25% larger than 20 meV reported previously in continuous films. The other is that the two coherence peaks appear asymmetric for most of the positions studied: They can either be positively [red curves in Fig. 2(b)] or negatively [blue curves in Fig. 2(b)] shifted in energy with respect to E_F.

Figure 3 summarizes the gap magnitude Δ and asymmetry δ for various positions and also for FeSe nanoflakes with varying A. The variations of both Δ and δ are found to be closely correlated to or fluctuate with A. A smaller flake usually leads to stronger variations in Δ and δ. These are reminiscent of the well-known shell effect in clean superconducting nanoparticles, such as Sn [10], which originates primarily from the discretization of the energy levels due to QSEs in small superconducting nanoparticles. In single UC FeSe films on $SrTiO_3$, recent ARPES measurements have revealed a relatively small Fermi wave vector $k_F \sim 0.2\pi/a$ for the electron pockets around M ($a = 0.38$ nm) [17–19]. This leads to a Fermi wavelength of $\lambda_F \sim 3.8$ nm and $k_F A^{0.5} \gg 1$, since A ranges from tens to hundreds of nm^2 in the FeSe nanoflakes investigated here. Compared to Sn [10], the larger λ_F in FeSe may result in enhanced quantum confinement effects. In the single UC FeSe nanoflakes studied, therefore, as the nanoflake is reduced to the nanoscale and is comparable to λ_F (e.g.,

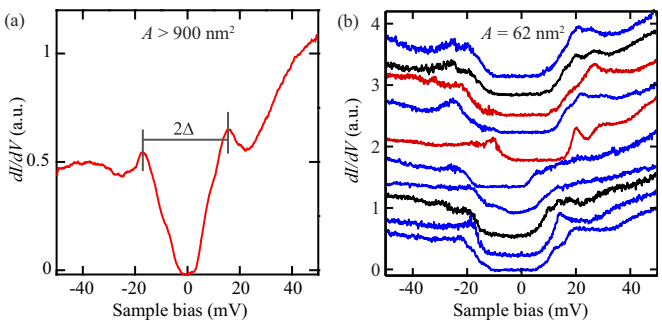

FIG. 2. (Color online) Comparison of dI/dV spectra acquired on single UC FeSe nanoflakes with different area A. (a) Typical differential conductance dI/dV spectrum in a large FeSe nanoflake ($A > 900$ nm^2). Two vertical gray lines indicate the energy positions of superconducting coherence peaks, with their separation defined as 2Δ. Tunneling gap is stabilized at $V_s = 50$ mV and $I = 95$ pA. (b) Normalized dI/dV spectra taken at equal separations ($\sim$0.8 nm) along a line of FeSe nanoflakes with $A = 62$ nm^2. Colored curves indicate the asymmetry of dI/dV spectra at various positions, signaling great spatial inhomogeneity. Here, we calculate 2Δ from the two strongest coherence peaks below and above E_F (not marked), respectively, in line with (a). The fine structures beyond the gaps may originate from QSE-resulted discrete energy levels.

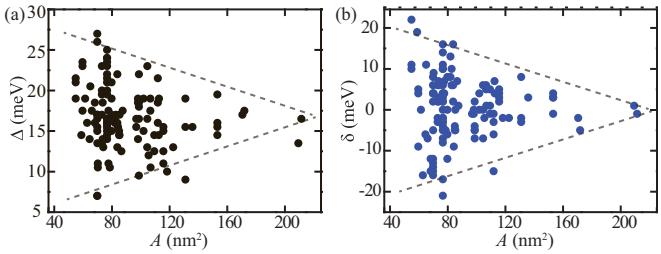

FIG. 3. (Color online) (a) Plot of gap magnitude Δ, and (b) gap asymmetry $\delta = \Delta_+ - \Delta_-$ vs FeSe nanoflake area A, with Δ_+ and Δ_- indicating the deviations of the two coherence peaks above and below E_F from E_F, respectively. Gray dotted lines are guides to the eye.

$A \lesssim 150$ nm^2), the lateral quantum confinement may become significant and result in a series of discrete energy levels, which will play a dominant role in Δ, with $k_F A^{0.5} \gg 1$ satisfied [10]. Depending on A and positions, the number of these discrete energy levels within the pairing energy region around E_F may fluctuate and also be strongly enhanced, leading to substantial changes in Δ (even exceeding the bulk value Δ_0), as observed here. Such an argument is also justified by observing the QSE-resulted fine peak structures beyond the near-E_F gap [Fig. 2(b)], which take little part in electron pairing and consequently superconductivity. Our study therefore provides direct evidence of QSEs in the layered superconductor FeSe.

The occurrence of lateral QSEs in single UC FeSe nanoflakes has been further solidified by taking STS on smaller nanoflakes, namely, $A < 40$ nm^2, below which Δ begins to increase in a prominent way. Figures 4(a) and 4(b) typify respectively the dI/dV spectra acquired on two FeSe nanoflakes with $A = 36$ and 27 nm^2, both indicating significant electron-hole asymmetry in the peak strength (>10). Furthermore, the gap magnitude Δ around E_F increases sharply with reducing A, regardless of its position in a specific FeSe nanoflake. This contrasts sharply with Δ fluctuation around 17 meV for the middle-sized FeSe nanoflakes ($40 \sim 150$ nm^2) [Fig. 3(a)], and also the theoretically predicated reduction in the superconducting gap Δ by QSE [9,10]. All these results, together with the extremely large Δ (up to ~80 meV for the smaller A investigated) in Fig. 4(c), suggest that the gap observed here may be not related to superconductivity, and that the superconductivity may be completely suppressed for small FeSe nanoflakes ($A \lesssim 40$ nm^2). Moreover, the dI/dV spectra in Figs. 4(a) and 4(b) show a series of discrete energy levels both above and below E_F, which was not observed in FeSe films [14]. The well-defined energy peaks characterize the formation of quantum well states (QWS) due to the lateral QSE. Figure 4(c) plots the energy separation ΔQWS between the highest occupied QWS (HOQWS) and lowest unoccupied QWS (LUQWS) as a function of A. Despite some scatter in the data, it is clear that Δ_{QWS} is anticorrelated with A, typical for QSEs. More significantly, below the critical FeSe nanoflake area of ~40 nm^2, Δ_{QWS} appears larger than the gap magnitude in Fig. 2, leading to a vanishing electron density of states (DOS) near E_F. Based on the Anderson criterion [28], it will kill the superconductivity, which is in excellent agreement with our experiment.

Having demonstrated the dependence of spectroscopic characteristics on FeSe nanoflake area A, one may wonder whether the asymmetric gap in Fig. 2 and discrete energy levels in Fig. 4 stem from the well-known Coulomb blockade (CB) in nanoscale tunnel junctions including the STM technique [29–32]. In CB effects, a series of pronounced peaks in dI/dV spectra with almost equal energy spacing are generated, which are little observed in middle-sized FeSe nanoflakes [Fig. 2]. Moreover, if the CB effects are involved and take sole responsibility for the gaps near E_F in Fig. 2, one should expect an increasing average gap magnitude with reducing A. This contrasts with our observations where the average Δ remains nearly constant [Fig. 3(a)]. In Fig. 4, despite several oscillations of the dI/dV peaks for smaller FeSe nanoflakes, their separations are not so equal. More significantly, we varied the tunneling separation and observed no dependence of the energies of the dI/dV peaks. These observations consistently rule out the possibility that the CB effects take responsibility for the observed peaks in the dI/dV spectra. Instead, we suggest that the asymmetric gaps in Fig. 2 may be superconductivity related and the dI/dV peaks in Fig. 4 originate from QSE, as argued above.

We finally comment on the distinction of QSEs observed here from those in Sn [10]. First, the gap magnitude Δ could be varied for a specific FeSe nanoflake [Fig. 2(b)], in sharp contrast to Sn nanoparticles [10]. One possible reason may stem from the difference in the superconducting coherence length ξ. In Sn, $\xi \sim 240$ nm is considerably larger than the size

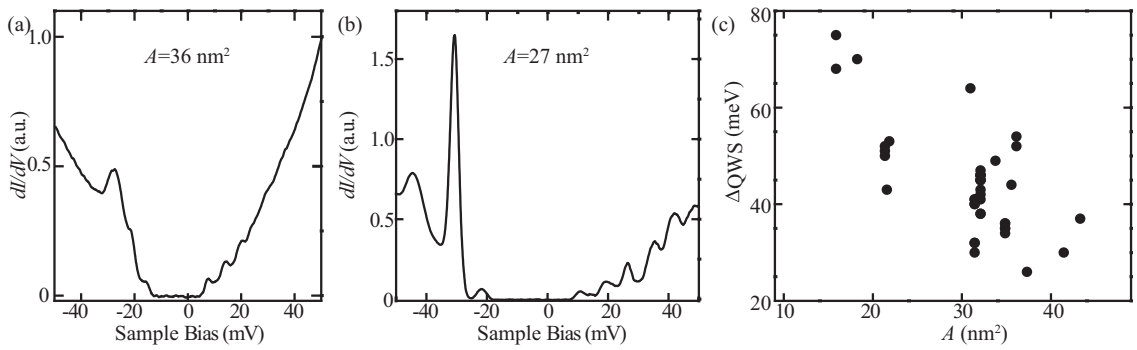

FIG. 4. (a), (b) dI/dV spectra on extremely small FeSe nanoflakes ($A < 40$ nm^2), which show distinct differences from those in larger FeSe nanoflakes ($A > 40$ nm^2). (c) Plot of HOQWS-LUQWS separation Δ_{QWS} as a function of FeSe nanoflake area A.

of the studied nanoparticles [33], from which Δ should change little with positions in a specific particle. However, ξ was found to be only 5.5 nm in thick FeSe films [34] and even smaller for single UC FeSe films due to the dimensionality effect. This appears smaller than the average lateral nanoflake size $A^{0.5}$ in Figs. 2 and 3. Therefore, the superconducting pairing, which depends on the local ($\sim\xi$) DOS, may alter with position in terms of possible variations in the local electron DOS. As a consequence, the superconductivity or gap magnitude Δ is expected to be site dependent. In addition, a recent theoretical study has demonstrated that the superconducting order parameter or pairing could be varied with position by an order of magnitude if the nanograins are highly symmetric [35]. This provides an alternative explanation for the observed gap inhomogeneity in FeSe nanoflakes, which does appear quite symmetric [Fig. 1(a)] in shape as compared to the Sn nanoparticles [10]. Second, the two coherence peaks in FeSe nanoflakes are asymmetric with respect to E_F [Fig. 3(b)], which is quite unexpected and distinct from the symmetric gaps in Sn nanoparticles as well. Further experimental and theoretical investigations are needed to fully understand these intriguing phenomena.

IV. SUMMARY

In summary, our detailed STM/STS study has revealed the QSEs in MBE-grown FeSe nanoflakes on a $SrTiO_3$ substrate. The superconductivity-related gap magnitude Δ could be varied and reaches a value of $\sim$25 meV as the area of the FeSe nanoflakes ranges from $\sim$40 to $\sim$150 nm^2. As A is further reduced, the superconductivity is completely suppressed due to strong QSEs. The present study opens up a way to exploit the QSEs on complex and layered unconventional superconductors.

ACKNOWLEDGMENTS

We thank T. Xiang for helpful conversations. This work was supported by the National Science Foundation and Ministry of Science and Technology of China. All STM images were processed by Nanotec WSXM software [36].

[1] Y. Guo, Y. F. Zhang, X. Y. Bao, T. Z. Han, Z. Tang, L. X. Zhang, W. G. Zhu, E. G. Wang, Q. Niu, Z. Q. Qiu, J. F. Jia, Z. X. Zhao, and Q. K. Xue, Science **306**, 1915 (2004).

[2] S. Y. Qin, J. Kim, Q. Niu, and C.-K. Shih, Science **324**, 1314 (2009).

[3] T. Zhang, P. Cheng, W. J. Li, Y. J. Sun, G. Wang, X. G. Zhu, K. He, L. Wang, X. C. Ma, X. Chen, Y. Y. Wang, Y. Liu, H. Lin, J. F. Jia, and Q. K. Xue, Nat. Phys. **6**, 104 (2010).

[4] A. Bezryadin, C. N. Lau, and M. Tinkham, Nature (London) **404**, 971 (2000).

[5] I. Giaever and H. R. Zeller, Phys. Rev. Lett. **20**, 1504 (1968).

[6] D. C. Ralph, C. T. Black, and M. Tinkham, Phys. Rev. Lett. **74**, 3241 (1995).

[7] J. von Delft, A. D. Zaikin, D. S. Golubev, and W. Tichy, Phys. Rev. Lett. **77**, 3189 (1996).

[8] A. A. Shanenko, M. D. Croitoru, M. Zgirski, F. M. Peeters, and K. Arutyunov, Phys. Rev. B **74**, 052502 (2006).

[9] C. T. Black, D. C. Ralph, and M. Tinkham, Phys. Rev. Lett. **76**, 688 (1996).

[10] S. Bose, A. M. García-García, M. M. Ugeda, J. D. Urbina, C. H. Michaelis, I. Brihuega, and K. Kern, Nat. Mater. **9**, 550 (2010).

[11] D. V. Averin and Y. V. Nazarov, Phys. Rev. Lett. **69**, 1993 (1992).

[12] A. M. García-García, J. D. Urbina, E. A. Yuzbashyan, K. Richter, and B. L. Altshuler, Phys. Rev. Lett. **100**, 187001 (2008).

[13] H. Olofsson, S. Åberg, and P. Leboeuf, Phys. Rev. Lett. **100**, 037005 (2008).

[14] Q. Y. Wang, Z. Li, W. H. Zhang, Z. C. Zhang, J. S. Zhang, W. LI, H. Ding, Y. B. Ou, P. Deng, K. Chang, J. Wen, C. L. Song, K. He, J. F. Jia, S. H. Ji, Y. Y. Wang, L. L. Wang, X. Chen, X. C. Ma, and Q. K. Xue, Chin. Phys. Lett. **29**, 037402 (2012).

[15] W. H. Zhang, Y. Sun, J. S. Zhang, F. S. Li, M. H. Guo, Y. F. Zhao, H. M. Zhang, J. P. Peng, Y. Xing, W. H. Chao, T. Fujita, A. Hirata, Z. Li, H. Ding, C. J. Tang, M. Wang, Q. Y. Wang, K. He, S. Ji, X. Chen, J. F. Wang, Z. C. Xia, L. Li, Y. Y. Wang, J. Wang, L. Wang, M. W. Chen, Q. K. Xue, and X. C. Ma, Chin. Phys. Lett. **31**, 017401 (2014).

[16] W. H. Zhang, Z. Li, F. S. Li, H. M. Zhang, J. P. Peng, C. J. Tang, Q. Y. Wang, K. He, X. Chen, L. Wang, X. C. Ma, and Q. K. Xue, Phys. Rev. B **89**, 060506 (2014).

[17] D. F. Liu, W. H. Zhang, D. X. Mou, J. F. He, Y. B. Ou, Q. Y. Wang, Z. Li, L. Wang, L. Zhao, S. L. He, Y. Y. Peng, X. Liu, C. Y. Chen, L. Yu, G. D. Liu, X. L. Dong, J. Zhang, C. T. Chen, Z. Y. Xu, J. P. Hu, X. Chen, X. C. Ma, Q. K. Xue, and X. J. Zhou, Nat. Commun. **3**, 931 (2012).

[18] S. L. He, J. F. He, W. H. Zhang, L. Zhao, D. F. Liu, X. Liu, D. X. Mou, Y. B. Ou, Q. Y. Wang, Z. Li, L. L. Wang, Y. Y. Peng, Y. Liu, C. Y. Chen, L. Yu, G. D. Liu, X. L. Dong, J. Zhang, C. T. Chen, Z. Y. Xu, X. Chen, X. C. Ma, Q. K. Xue, and X. J. Zhou, Nat. Mater. **12**, 605 (2013).

[19] S. Y. Tan, Y. Zhang, M. Xia, Z. Ye, F. Chen, X. Xie, R. Peng, D. F. Xu, Q. Fan, H. C. Xu, J. Jiang, T. Zhang, X. C. Lai, T. Xiang, J. P. Hu, N. P. Xie, and D. L. Feng, Nat. Mater. **12**, 634 (2013).

[20] J. Bang, Z. Li, Y. Y. Sun, A. Samanta, Y. Y. Zhang, W. H. Zhang, L. Wang, X. Chen, X. C. Ma, Q. K. Xue, and S. B. Zhang, Phys. Rev. B **87**, 220503 (2013).

[21] R. Peng, X. P. Shen, X. Xie, H. C. Xu, S. Y. Tan, M. Xia, T. Zhang, H. Y. Cao, X. G. Gong, J. P. Hu, B. P. Xie, and D. L. Feng, Phys. Rev. Lett. **112**, 107001 (2014).

[22] J. F. Ge, Z. L. Liu, C. Liu, C. L. Gao, D. Qian, Q. K. Xue, Y. Liu, and J. F. Jia, Nat. Mater., doi:10.1038/nmat4153 (2014).

[23] M. A. N. Araújo, A. M. García-García, and P. D. Sacramento, Phys. Rev. B **84**, 172502 (2011).

[24] S. Mishra, K. Song, J. A. Koza, and M. Nath, ACS Nano **7**, 1145 (2013).

[25] S. Mishra, K. Song, K. C. Ghosh, and M. Nath, ACS Nano **8**, 2077 (2014).

[26] C. L. Song, Y. L. Wang, Y. P. Jiang, Z. Li, L. Wang, K. He, X. Chen, X. C. Ma, and Q. K. Xue, Phys. Rev. B **84**, 020503 (2011).

[27] Z. Li, J. P. Peng, H. M. Zhang, W. H. Zhang, H. Ding, P. Deng, K. Chang, C.-L. Song, S. H. Ji, L. Wang, K. He, X. Chen, Q. K. Xue, and X. C. Ma, J. Phys.: Condens. Matter **26**, 265002 (2014).

[28] P. W. Anderson, J. Phys. Chem. Solids **11**, 26 (1959).

[29] P. J. M. van Bentum, R. T. M. Smokers, and H. van Kempen, Phys. Rev. Lett. **60**, 2543 (1988).

[30] M. Amman, R. Wilkins, E. Ben-Jacob, P. D. Maker, and R. C. Jaklevic, Phys. Rev. B **43**, 1146 (1991).

[31] M. Amman, S. B. Field, and R. C. Jaklevic, Phys. Rev. B **48**, 12104 (1993).

[32] Z. F. Zhong, H. L. Shen, R. X. Cao, L. Sun, K. P. Li, J. Hu, Z. Liu, D. Wu, X. R. Wang, and H. F. Ding, Phys. Rev. B **88**, 125408 (2013).

[33] C. Kittel and P. McEuen, *Introduction to Solid State Physics* (Wiley, New York, 1976), Vol. 8.

[34] C. L. Song, Y. L. Wang, Y. P. Jiang, L. Wang, K. He, X. Chen, J. E. Hoffman, X. C. Ma, and Q. K. Xue, Phys. Rev. Lett. **109**, 137004 (2012).

[35] M. D. Croitoru, A. A. Shanenko, C. C. Kaun, and F. M. Peeters, Phys. Rev. B **83**, 214509 (2011).

[36] I. Horcas, R. Fernandez, J. M. Gomez-Rodriguez, J. Colchero, J. Gómez-Herrero, and A. M. Baro, Rev. Sci. Instrum. **78**, 013705 (2007).